# Real-Time Maximum Power Point Tracking Method Based on Three Points Approximation by Digital Controller for PV System

**Seung-Tak Kim\*, Tae-Ho Bang\*, Seong-Chan Lee\* and Jung-Wook Park**[†]

**Abstract** – This paper proposes the new method based on the availability of three points measurement and convexity of photovoltaic (PV) curve characteristic at the maximum power point (MPP). In general, the MPP tracking (MPPT) function is the important part of all PV systems due to their power-voltage (P-V) characteristics related with weather conditions. Then, the analog-to-digital converter (ADC) and low pass filter (LPF) are required to measure the voltage and current for MPPT by the digital controller, which is used to implement the PV power conditioning system (PCS). The measurement and quantization error due to rounding or truncation in ADC and the delay of LPF might degrade the reliability of MPPT. To overcome this limitation, the proposed method is proposed while improving the performances in both steady-state and dynamic responses based on the detailed investigation of its properties for availability and convexity. The performances of proposed method are evaluated with the several case studies by the PSCAD/EMTDC® simulation. Then, the experimental results are given to verify its feasibility in real-time.

**Keywords**: Analog-to-digital converter, Low pass filter, Maximum power point tracking (MPPT), Photovoltaic (PV) power system.

## 1. Introduction

In recent, the photovoltaic (PV) generation has become more important among several renewable energy sources worldwide. In particular, the output characteristics of PV array are always varying with the weather conditions such as irradiation level and atmospheric temperature. Then, its optimal operating condition must be considered to produce the maximum power. Therefore, the maximum power point tracking (MPPT) function of all PV systems has been the important part when they are applied in practice.

Many techniques for MPPT have been proposed and implemented. Most MPPT methods use the voltage and current from PV array, and some methods exploit the temperatures, irradiance, and load conditions. In particular, the fractional open-circuit voltage and short-circuit current strategy provides the simple and effective way to obtain the maximum power [1]. However, periodical disconnection or short-circuit is required to measure the voltage or current for reference. This results in increasing more power loss [2]. Also, the hill climbing and incremental conductance method [3] uses the derivatives of power or current based on the fact that the sign of derivative is changed on the either side of peak [4]. The neural network (NN)-based MPPT controller improves the tracking efficiency by utilizing the multilayer control structure [5, 6]. The

extremum seeking control (ESC) [7, 8] is proposed with the nearly model-free and self-optimizing control strategy. Other MPPT methods based on the downward parabola [9] and modified particle swarm optimization (PSO) algorithm [10] have been proposed.

Among various MPPT methods, the perturbation and observation (P&O) method [11, 12] has been widely applied in industry because it can be easily implemented in digital controller. However its perturbing process still continues even when it reaches the optimal operating point in a steady-state condition. Then, it might cause the extra energy loss and system instability while performing the MPPT process. In general, the perturbation of operating voltage can be well captured in a rapidly changing weather condition. However, the P&O method has the low performance during cloudy days. This sometimes leads to the wrong tracking direction from its MPP.

The analog-to-digital converter (ADC) and low pass filter (LPF) are required to measure the voltage and current from PV system in real-time. Also, they are widely used in the power conditioning system (PCS). The practical measurement and quantization error due to rounding or truncation in ADC and the delay of LPF might degrade the reliability of MPPT in practice. To overcome this limitation, this paper proposes the new real-time MPPT method based on the availability of measurement at three points and the convexity of power-voltage (P-V) curve at MPP. Then, its performances are evaluated by both the power system computer aided design/electromagnetic transients including DC (PSCAD/EMTDC®) based time-domain simulation and experimental tests.

†  Corresponding Author: School of Electrical and Electronic Engineering, Yonsei University, Seoul, Korea (jungpark@yonsei.ac.kr)
\*  School of Electrical and Electronic Engineering, Yonsei University, Seoul, Korea ({miso2me, thbang2018, lee012}@yonsei. ac.kr)

## 2. Properties of PV Array

### 2.1 Availability

In general, the PV array consists of many PV cells, which are connected in serial and parallel structures. Then, it is characterized by the single diode model, which is based on the modified Shockley-diode equation, as shown in Fig. 1. Also, its current can be calculated as (1) [13].

$$I_s = I_{sc} - I_O \left( e^{\frac{V_s + I_s \cdot R_s}{n \cdot N_s \cdot V_T}} - 1 \right) - \frac{V_s + I_s \cdot R_s}{R_p} \quad (1)$$

where $I_s$ is the output current of PV module, $I_{SC}$ is the short circuit current, $I_O$ is the diode saturation current, $n$ is the ideal constant of diode, $V_s$ is the thermal voltage of PV module, $R_s$ is the series resistance, $R_p$ is the parallel resistance, $V_T$ is the thermal potential of a PV cell, and $N_s$ is the number of series connections of a PV cell [14]. Then, the voltage and current of PV array are required to calculate its output power. The ADC is required for the use of digital signal processor (DSP) in implementation of PV PCS. As mentioned in previous, the practical measurements might have the errors due to noises as well as the quantization, non-linearity, and signal-dependent mismatches. In order to reduce these errors, the LPF is applied to the measurements. The feature of LPF correlates with its bandwidth, and it has the signal delay. Then, the output power of PV array, $P_{PV}$ is calculated as

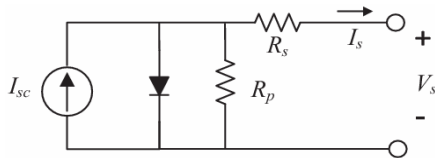$$P_{PV} = V_{PV} \cdot I_{PV} \quad (2)$$



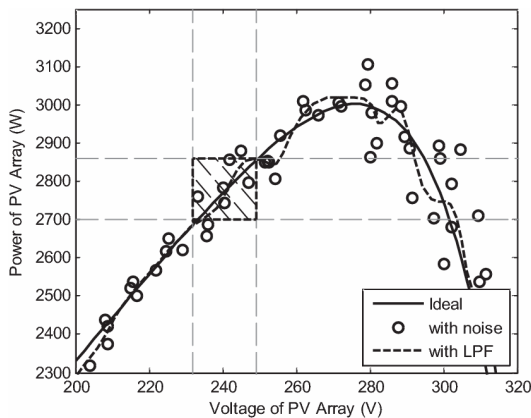**Fig. 1.** The equivalent circuit of PV array.



**Fig. 2.** The P-V characteristic curve and the availability of measurement data.

where $V_{PV}$ and $I_{PV}$ are measured from PV array by using the ADC and LPF. In this study, the data availability in real-time is investigated. Fig. 2 shows the P-V characteristic curve and the availability of measurement data. The rectangular box filled with diagonal lines indicates the availability area of one measurement point. If the next measurement point is in the boundary of rectangular, which is available to select it by considering the measurement error range, the point is ignored due to the noise and error effects. Otherwise, if it is strictly outside of this boundary, the point is accepted as the one of measurement point.

### 2.2 Convexity

As shown in Fig. 2, the P-V characteristic curve of PV array is convex to upward. Therefore, the curve can be estimated as a quadratic function at close to MPP. If three discrete points $[(V_{n-2}, P_{n-2}), (V_{n-1}, P_{n-1}),$ and $(V_n, P_n)]$ are located in the vicinity of peak, the coefficients, $c_1$ and $c_2$ of quadratic function with the interpolation polynomial are given by

$$c_1 = \frac{P_{n-1} - P_n}{V_{n-1} - V_n} \quad (3)$$

$$c_2 = \frac{P_{n-2} - \left( P_n + c_1 \cdot \left( V_{n-1} - V_n \right) \right)}{\left( V_{n-2} - V_{n-1} \right)\left( V_{n-2} - V_n \right)} \quad (4)$$

If the sign of $c_2$ is negative, the quadratic curve becomes convex to upward. Then, the MPPs corresponding to three points are obtained as

$$V_{MPP} = -\frac{c_1 - c_2 \cdot \left( V_{n-1} + V_n \right)}{2 \cdot c_2} \quad (5)$$

$$P_{MPP} = P_n + c_1 \left( V_{MPP} - V_n \right) \\ + c_2 \left( V_{MPP} - V_n \right)\left( V_{MPP} - V_{n-1} \right) \quad (6)$$

where $V_{MPP}$ and $P_{MPP}$ are the estimated voltage and power of MPP, respectively.

Unfortunately, when the three points are located far away from the MPP, the estimated peak value might indicate the wrong point, as shown in Figs. 3(a) and 3(b). For example, assume that three points include some error in the first time, as shown in Fig. 3(a). Then, even though the estimated quadratic curve is convex to upward, its peak point is not MPP. Next, the new point is measured out of availability boundary, and the oldest point is removed from previous set of three measured points. Also, the number of points is re-arranged in time order. However, the shape of estimated curve becomes concave without the maximum point, as shown in Fig. 3(b). Finally, the point is measured as shown in Fig. 3(c). The power of latest point is between those of other two points. This means that three measured points are not biased to one side slope. Therefore, the estimated voltage and power of MPP is the same as those
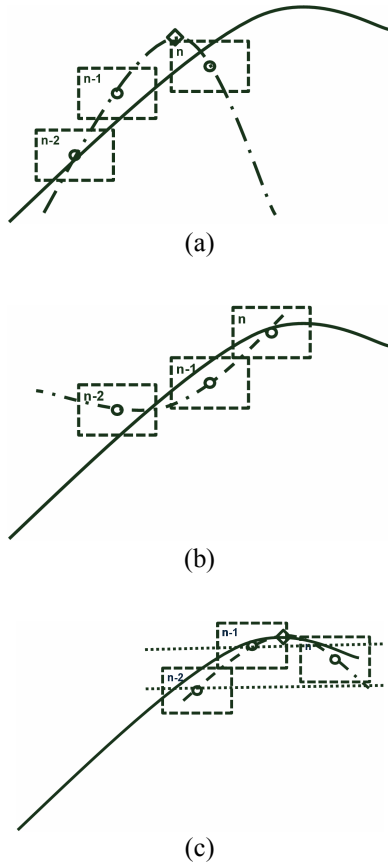
(a)

(b)

(c)

**Fig. 3.** The estimation of quadratic curve: (a) wrong peak estimation; (b) concave curve, and (c) accurate peak estimation.

of original MPP.

## 3. Proposed MPPT Algorithm

The flowchart of proposed real-time MPPT algorithm by using three points approximation is shown in Fig. 4. Firstly, it measures and calculates the current, voltage, and output power of PV array. Then, it grasps the availability of measurements as described in Section 2.1. If they satisfy the condition for availability, it removes the oldest point and re-arranges the data set of three point measurements.

Next, the proposed algorithm determines if a quadratic function with convex property can be formed even when it rarely occurs. Thereafter, if voltages at all three points are same, the reference voltage of MPPT controller, the $V_{ref}$ is decreased by the inertia voltage, $V_{INR}$. This means that three points are in the right side of PV curve, which has steep slope. And, the $V_{INR}$ is calculated by (7) with the availability voltage, $V_{ava}$ and the control error voltage, $V_{cerr}$ if controller has the steady-state error at new measurement point, which satisfies the availability condition.
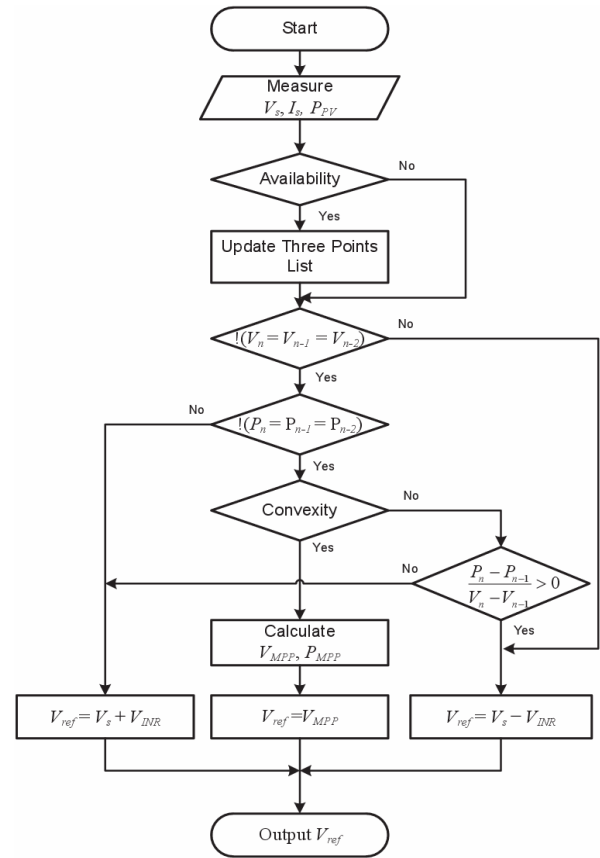
$$V_{INR} = V_{ava} + V_{cerr} \tag{7}$$



**Fig. 4.** The flowchart of proposed MPPT algorithm.

On the other hand, if powers at all three points are same, the $V_{ref}$ is increased by $V_{INR}$. This means that three points are in the left side of PV curve, which has gradual slope. Then, it decides whether the sign of $c_2$ from (4) is less than zero and whether the point is close to the peak for the convexity of estimated quadratic curve, as given by (8).

$$\left( \left( V_n < V_{n-1} < V_{n-2} \right) \text{ or } \left( V_{n-2} < V_{n-1} < V_n \right) \right) \\ \text{and } \left( P_{n-2} < P_n < P_{n-1} \right) \tag{8}$$

When the estimated quadratic curve is not convex, the $V_{INR}$ varies depending on the derivative of power as

$$\frac{P_n - P_{n-1}}{V_n - V_{n-1}} > 0 \tag{9}$$

Otherwise, the $V_{ref}$ becomes the $V_{MPP}$ by (5). Finally, it is used as the input of MPPT controller in real-time.

## 4. Simulation Results

### 4.1 System configuration

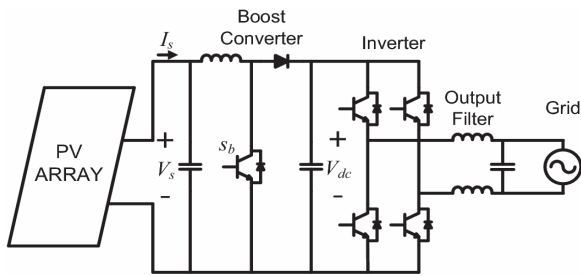The performance of proposed method is firstly evaluated

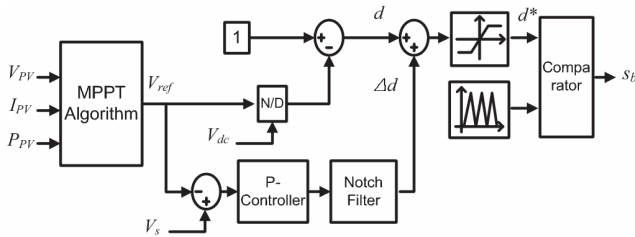**Fig. 5.** Structure of two-stage grid-connected PV PCS



**Fig. 6.** Block diagram of boost control for MPPT.

by simulation based on the PSCAD/EMTDC® software. The PV PCS of 3 kW in Fig. 5 consists of a DC/DC boost converter and a full-bridge pulse-width-modulation (PWM) inverter with the switching frequency of 20 kHz. The boost converter performs the voltage amplification and MPPT. To obtain the high-quality output, the inverter should provide the tight voltage regulation by controlling its output current in phase with the utility voltage and therefore obtaining the unity power factor.

The boost converter controller for MPPT might have the LC resonance component. In this case, the notch filter in Fig. 6 can reduce the effect of resonance between outputs of PV arrays and boost converter [15].
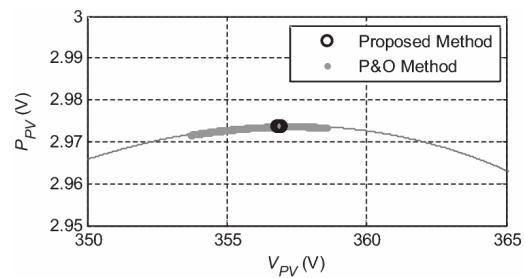
### 4.2 Simulation results

The simulation results are shown in Fig. 7. The initial insolation and temperature are 0.9 kW/m$^2$ and 15 ℃, respectively. Assume that the entire array receives uniform insolation. The corresponding voltage, $V_{PV}$ at MPP is 357.3 V. At 0.2 s, a sudden change in environmental condition occurs. In other words, the insolation and temperature are increased to 0.35 kW/m$^2$ and 25℃, respectively. Then, the value of $V_{PV}$ is changed to 327.7 V. At 0.4 s, the external condition is restored to its initial one. Note that when the output power from PCS is 3 kW, its nominal voltage is 356.8 V. If the PV array generates 1 kW, the operating voltage of PCS is 327.7 V.
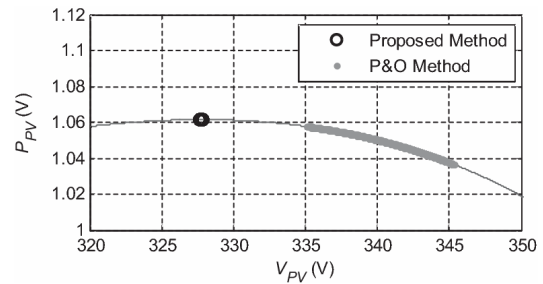
The dynamic performances of proposed MPPT method and P&O method are compared in Fig. 7(a). The voltage by P&O method shows the serious oscillatory response around the MPP in the range from 0.2 s to 0.4 s. From Figs. 7(b) and 7(b), it is clearly observed that the P&O method is tracking the incorrect operating points. This behavior becomes more serious in the range from 0.2 s to 0.4 s
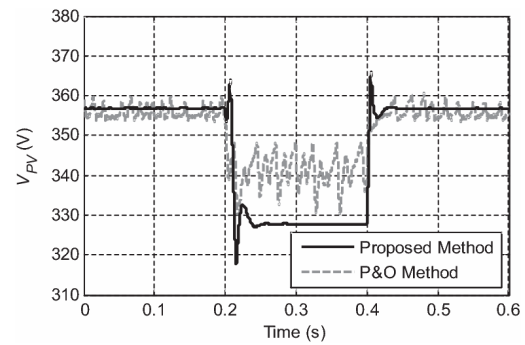


(a)



(b)



(c)

**Fig. 7.** Simulation results: (a) Voltage response; (b) P-V curve at 0.9 kW/m$^2$ and 15℃, and (c) P-V curve at 0.35 kW/m$^2$ and 25℃.

**Table 1.** Comparison results for MPPT error and efficiency

| Method | Operating voltage | Average voltage | MPPT error | Output power | MPPT efficiency |
|---|---|---|---|---|---|
| **Proposed** | **356.8 - 356.9 V** | **356.8 V** | **0.13 %** | **2973 W** | **99.99 %** |
| P&O | 353.6 -358.5 V | 355.7 V | 0.43 % | 2972 W | 99.96 % |
| **Proposed** | **327.7 - 327.8 V** | **327.7 V** | **0.01 %** | **1061 W** | **99.99 %** |
| P&O | 335.1 -345.4 V | 340.8 V | 3.99 % | 1046 W | 98.60 % |

due to effect of error by ADC and LPF. In contrast, the proposed MPPT method provides the exact MPPT performance while there are no oscillations in steady-state conditions.

The comparison results for MPPT error and efficiency are given in Table 1. It is observed that the proposed MPPT outperforms the P&O method. In particular, when the PV output power is low, the proposed method provides the very accurate performance with the error of 0.01 %, which is extremely less than 3.99 % by P&O method.
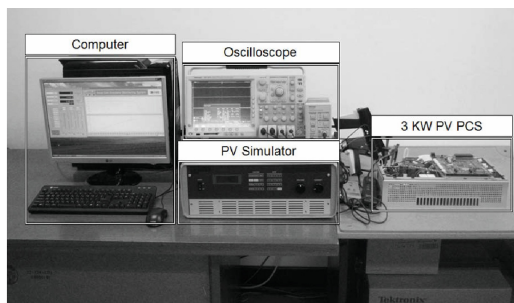
## 5. Experimental Results

### 5.1 Hardware implementation

The effectiveness of proposed real-time MPPT method is verified by the experimental test implemented in hardware, as shown in Fig. 8(a). The photograph of real PV PCS of 3 kW is shown in Fig. 8(b). The DC/DC boost converter and inverter are independently operated with the switching frequency of 20 kHz. In particular, their PWM controllers are implemented by the digital signal processor (DSP) of TMS320F2812. Then, the boost converter performs the MPPT algorithm. The inverter is connected to a commercial electrical outlet of 220 V. Also, it controls the DC capacitor voltage in real-time.
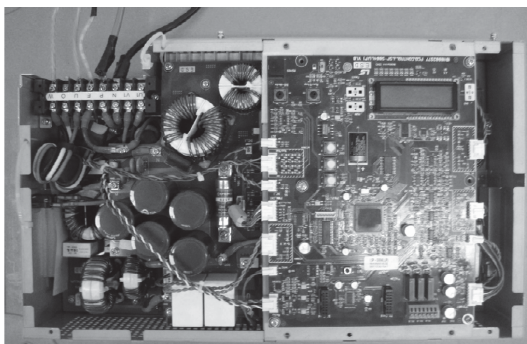
The voltage and current of PV simulator are measured using the digital phosphor Tektronix oscilloscope of the DPO4054. Also, its output power is measured from the power analysis application module of DPO4PWR, which is attached to the oscilloscope of DPO4054.

### 5.2 Experimental results

The step change of $V_{ref}$ is applied at 80 s and 240 s to observe the voltage responses. Before 80 s, the output power from PV simulator is 3 kW. Thereafter, it generates the output power of 1 kW. At 240 s, it is restored to the initial 3 kW. When the PV output powers are 3 kW and 1 kW, the corresponding MPP voltages are 290 V and 240 V,
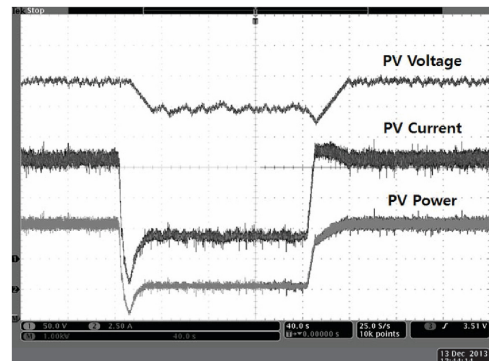
respectively. Also, the MPPT algorithm operates per 1 s in order to take account of ADC sampling and digital LPF calculation, and to make sure of system stability.
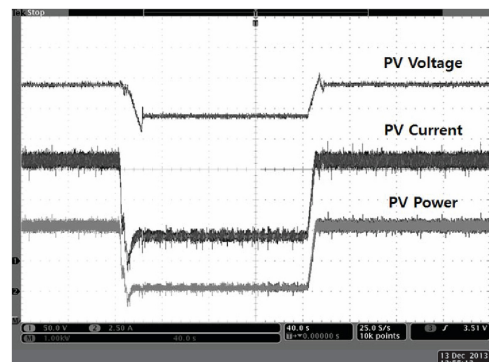
The experimental results are shown in Fig. 9. When the P&O method is applied to the PCS, it is clearly shown from Fig. 9 (a) that the $V_s$ oscillates between 238.5 V and 256.0 V in the range from 80 s to 240 s. However, this large variation is dramatically reduced by the proposed method, as shown in Fig. 9 (b). Also, even before the operating condition is changed at 1 s, the voltage variation by the P&O method is between 285.9 V and 296.3. However, that by the proposed method varies only between 288.3 V to 289.7 V.

Moreover, the P&O and proposed methods require 35-40 and 20-23 steps in DSP for the PV system to reach the MPP, respectively. The above all results clearly verify the better dynamic performance of proposed real-time MPPT method.

The P-V curve analysis of experimental results is shown in Fig 10. Also, the experimental results for MPPT error and efficiency by two MPPT methods are compared in Table 2. It is observed that the MPPT performance of proposed MPPT method is better than that of P&O method. In particular, the average value of output power by the proposed method is greater than that by P&O method in both conditions. This means that the proposed MPPT method is more suitable under various operating conditions



(a)



(b)

**Fig. 8.** Hardware implementation: (a) hardware set-up for experimental test and (b) PV PCS of 3 kW.



(a)



(b)

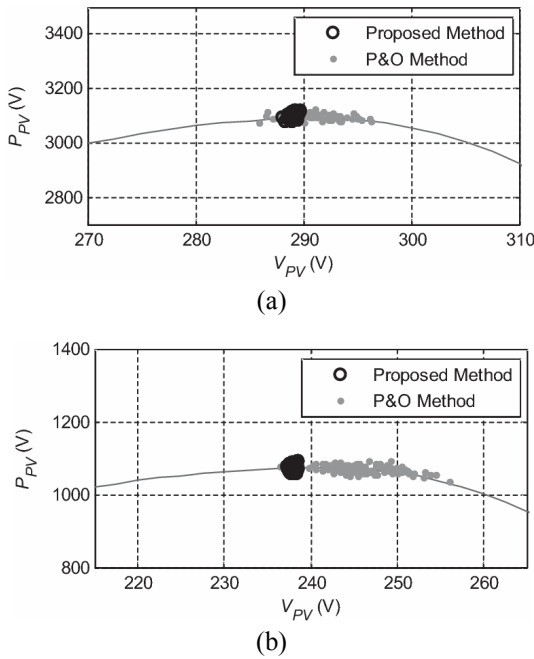**Fig. 9.** Experimental results: (a) P&O method and (b) proposed method.

**Fig. 10.** P-V curve analysis of experimental results: (a) for PV power of 3 kW and (b) for PV power of 1 kW.

**Table 2.** Comparison results by experiment test

| Method | Operating voltage | Average voltage | MPPT error | Output power | MPPT efficiency |
|---|---|---|---|---|---|
| **Proposed** | **288.3 - 289.7 V** | **289.1 V** | **0.30 %** | **3103 W** | **99.13 %** |
| P&O | 285.9 -296.3 V | 291.1V | 0.39 % | 3098 W | 98.97 % |
| **Proposed** | **237.3 - 238.5 V** | **237.9 V** | **0.87 %** | **1074 W** | **98.22 %** |
| P&O | 238.5 -256.0 V | 246.3 V | 2.65 % | 1070 W | 97.88 % |

in practice.

## 6. Conclusion

This paper proposed the new real-time maximum power point tracking (MPPT) method based on the availability of three points measurements and convexity of power-voltage (P-V) characteristic curve. The performance of proposed MPPT method was evaluated by both simulation study and experimental test with the practical photovoltaic (PV) power conditioning system (PCS) of 3 kW, which was implemented in hardware.

Both simulation and experimental results verified that the proposed method can improve the performances of both steady-state and dynamic responses effectively. It would be expected that the proposed method can be preferably used in practice.

## Acknowledgements

## References

[1] M. A. S. Masoum, H. Dehbonei, and E. F. Fuchs, "Theoretical and experimental analyses of photo-voltaic systems with voltage and current-based maximum power-point tracking," *IEEE Trans. Energy Convers.*, vol. 17, no. 4, pp. 514-522, Dec. 2002.

[2] F. Liu, S. Duan, F. Liu, B. Liu, and Y. Kang, "A variable step size INC MPPT method for PV systems," *IEEE Trans. Ind. Electron.*, vol. 55, no. 7, pp. 2622-2628, Jul. 2008.

[3] S. Kjaer, "Evaluation of the "hill climbing" and the "incremental conductance" maximum power point trackers for photovoltaic power systems," *IEEE Trans. Energy Convers.*, vol. 27, no. 4, pp. 922-929, Dec. 2012.

[4] A. Safari and S. Mekhilef, "Simulation and hardware implementation of incremental conductance MPPT with direct control method using cuk converter," *IEEE Trans. Ind. Electron.*, vol. 58, no. 4, pp. 1154-1161, Apr. 2011.

[5] W. M. Lin, C. M. Hong, and C. H. Chen, "Neural-network-based MPPT control of a stand-alone hybrid power generation system," *IEEE Trans. Power Electron.*, vol. 26, no. 12, pp. 3571-3581, Dec. 2011

[6] M. Veerachary, T. Senjyu, and K. Uezato, "Neural-network-based maximum-power-point tracking of coupled-inductor interleaved-boost converter-supplied PV system using fuzzy controller," *IEEE Trans. Ind. Electron.*, vol. 50, no. 4, pp. 749-758, Aug. 2003.

[7] S. L. Brunton, C. W. Rowley, S. R. Kulkarni, and C. Clarkson, "Maximum power point tracking for photo-voltaic optimization using ripple-based extremum seeking control," *IEEE Trans. Power Electron.*, vol. 25, no. 10, pp. 2531-2540, Oct. 2010.

[8] X. L,I, Y. Li, and J. E. Seem, "Maximum power point tracking for photovoltaic system using adaptive extremum seeking control," *IEEE Trans. Control Syst. Tech.*, vol. 21, no. 6, pp. 2315-2322, Nov. 2013

[9] F.-S. Pai, R.-M. Chao, S. H. Ko, and T.-S. Lee, "Performance evaluation of parabolic prediction to maximum power point tracking for PV array," *IEEE Trans. Sustain. Energy*, vol. 2, no. 1, pp. 60-68, Jan. 2011.

[10] K. Ishaque, Z. Salam, M. Amjad, and S. Mekhilef "An improved particle swarm optimization (PSO)-based MPPT for PV with reduced steady state oscillation," *IEEE Trans. Power Electron.*, vol. 27, no. 8, pp. 3627-3638, Aug. 2012

[11] M. A. Elgendy, B. Zahawi, and D. J. Atkinson, "Assessment of perturb and observe MPPT algorithm implementation techniques for PV pumping applications," *IEEE Trans. Sustain. Energy*, vol. 3, no. 1, pp. 21-33, Jan. 2012.

[12] N. Femia, G. Petrone, G. Spagnuolo and M. Vitelli,

"Optimization of perturb and observe maximum power point tracking method," *IEEE Trans. Power Electron.*, vol. 20, no. 4, pp. 963-973, Jul. 2005

[13] S. Liu and R. A. Dougal, "Dynamic multiphysics model for solar array," *IEEE Trans. Energy Conv.*, vol. 17, no. 2, pp. 285-294, Jun. 2002.

[14] J. J. Soon and K. S. Low, "Photovoltaic model identification using particle swarm optimization with inverse barrier constraint," *IEEE Trans. Power Electron.*, vol. 27, no. 9, pp. 3975-3983, Mar. 2012

[15] S.-T. Kim and J.-W. Park "Improvement of boost converter control using notch filter for PV system," in *Proc. 2014 Int. Conf. on Electronics, Information and Communications (ICEIC)*, Kota Kinabalu, Malaysia Jan. 2014.

**Seung-Tak Kim** received the B.S. degree from School of Electrical and Electronic Engineering from Yonsei University, Seoul, Korea, in 2009, where he is currently pursuing the Ph.D. degree. His research interests are in control of renewable energies based systems, hardware implementation of grid-connected inverter with photovoltaic and energy storage devices, and energy management system for stabilization of distributed generation systems.

**Tae-Ho Bang** received the B.S. degree from the School of Electrical and Electronic Engineering, Yonsei University, Seoul, Korea, in 2013.He is currently working toward the Ph.D. degree in the combined M.S. and Ph.D. program at Yonsei University. His research interests include hardware implementation of grid-connected inverter with photovoltaic and energy storage devices, and energy management system for stabilization of distributed generation systems.

**Seong-Chan Lee** received the B.S. degree from the School of Electrical and Electronic Engineering, Yonsei University, Seoul, Korea, in 2013. He is currently working toward the M.S degree at Yonsei University. His research interests include active cell balancing in BMS and hardware implementation of active cell balancing.

**Jung-Wook Park** was born in Seoul, Korea. He received the B.S. degree (summa cum laude) from the Department of Electrical Engineering, Yonsei University, Seoul, Korea, in 1999, and the M.S.E.C.E. and Ph.D. degrees from the School of Electrical and Computer Engineering, Georgia Institute of Technology, Atlanta, USA in 2000 and 2003, respectively. He was a Post-doctoral Research Associate in the Department of Electrical and Computer Engineering, University of Wisconsin, Madison, USA during 2003-2004, and a Senior Research Engineer with LG Electronics Inc., Korea during 2004-2005. He is currently an Associate Professor in the School of Electrical and Electronic Engineering, Yonsei University, Seoul, Korea. He is now leading the National Leading Research Laboratory (NLRL) designated by Korea government to the subject of integrated optimal operation for smart grid. He is also a chair of Yonsei Power and Renewable Energy FuturE technology Research Center (Yonsei-PREFER) in School of Electrical and Electronic Engineering, Yonsei University, Seoul, Korea. His current research interests are in power system dynamics, renewable energies based distributed generations, power control of electric vehicle, and optimization control algorithms. Prof. Park was the recipient of Second Prize Paper Award in 2003 from Industry Automation Control Committee, Prize Paper Award in 2008 from Energy Systems Committee of the IEEE Industry Applications Society (IAS), and Young Scientist Presidential Award in 2013 from the Korean Academy of Science and Technology (KAST) and the Ministry of Science, ICT, and Future Planning, Korea.